IL-6 exhibits both *cis*- and *trans*-signaling in osteocytes and osteoblasts, but only *trans*-signaling promotes bone formation and osteoclastogenesis

Received for publication, February 21, 2019, and in revised form, March 25, 2019 Published, Papers in Press, March 28, 2019, DOI 10.1074/jbc.RA119.008074

Narelle E. McGregor[‡], Melissa Murat[‡§1], Jeevithan Elango[‡¶2], Ingrid J. Poulton[‡], Emma C. Walker[‡], Blessing Crimeen-Irwin[‡], Patricia W. M. Ho[‡], Jonathan H. Gooi[‖], T. John Martin[‡‖], and Natalie A. Sims[‡‖3]**

*From the [‡]Bone Cell Biology and Disease Unit, St. Vincent's Institute of Medical Research, Melbourne, Victoria 3065, Australia, the [¶]Department of Marine Bio-Pharmacology, College of Food Science and Technology, Shanghai Ocean University, Shanghai 201306, China, the [§]Department of Physiology, Anatomy, and Microbiology, La Trobe University, Bundoora, Victoria 3086, Australia, the [‖]Department of Medicine, University of Melbourne, St. Vincent's Hospital, Melbourne, Victoria 3065, Australia, and the **Structural Biology Unit, St. Vincent' s Institute of Medical Research, Melbourne, Victoria 3065, Australia*

Edited by Alex Toker

Interleukin 6 (IL-6) supports development of bone-resorbing osteoclasts by acting early in the osteoblast lineage via membrane-bound (*cis*) or soluble (*trans*) receptors. Here, we investigated how IL-6 signals and modifies gene expression in differentiated osteoblasts and osteocytes and determined whether these activities can promote bone formation or support osteoclastogenesis. Moreover, we used a genetically altered mouse with circulating levels of the pharmacological IL-6 *trans*-signaling inhibitor sgp130-Fc to determine whether IL-6 *trans*-signaling is required for normal bone growth and remodeling. We found that IL-6 increases suppressor of cytokine signaling 3 (*Socs3*) and CCAAT enhancer-binding protein δ (*Cebpd*) mRNA levels and promotes signal transducer and activator of transcription 3 (STAT3) phosphorylation by both *cis*- and *trans*-signaling in cultured osteocytes. In contrast, RANKL (*Tnfsf11*) mRNA levels were elevated only by *trans*-signaling. Furthermore, we observed soluble IL-6 receptor release and ADAM metallopeptidase domain 17 (ADAM17) sheddase expression by osteocytes. Despite the observation that IL-6 *cis*-signaling occurs, IL-6 stimulated bone formation *in vivo* only via *trans*-signaling. Although IL-6 stimulated RANKL (*Tnfsf11*) mRNA in osteocytes, these cells did not support osteoclast formation in response to IL-6 alone; binucleated TRAP+ cells formed, and only in response to *trans*-signaling. Finally, pharmacological, sgp130-Fc–mediated inhibition of IL-6 *trans*-signaling did not impair bone growth or remodeling unless mice had circulating sgp130-Fc levels > 10 μg/ml. At those levels, osteopenia and impaired bone growth occurred, reducing bone strength. We conclude that high sgp130-Fc levels may have detrimental off-target effects on the skeleton.

IL-6[4] is a major pro-inflammatory cytokine that stimulates formation of bone-resorbing osteoclasts *in vitro* (1) and in bone-destructive conditions such as Paget's disease of bone (2), estrogen deficiency (3, 4), colitis (5), inflammatory arthritis (6, 7), and multiple myeloma (8).

IL-6 has two modes of action: *cis* and *trans* (9). Classic (*cis*)-signals occur only in cells expressing membrane-bound IL-6 receptor (IL-6R); in *cis*-signaling, IL-6 binds membrane-bound IL-6R and then recruits a glycoprotein 130 (gp130) homodimer, which initiates intracellular signaling. The second mode is *trans*-signaling, where IL-6 binds to soluble IL-6R (sIL-6R), either provided locally or via the circulation, before recruiting the gp130 homodimer. This additional mechanism allows IL-6 to influence cells lacking IL-6R and amplifies its effects in IL-6R– expressing cells (9).

Although osteoclasts and their progenitors express IL-6R (10), IL-6 does not stimulate osteoclast formation by direct action on osteoclast progenitors. IL-6, like other cytokines and endocrine factors, such as oncostatin M, IL-1, parathyroid hormone, and 1,25-dihydroxyvitamin D_3, stimulates osteoclast formation indirectly by acting on early osteoblast lineage cells (1, 11). These cells respond by producing the membrane-bound protein RANKL (12, 13), which promotes osteoclast differentiation by binding to RANK on osteoclast precursors. In the case of IL-6, osteoclast precursors co-cultured with early osteoblast lineage cells differentiate to osteoclasts only if recombinant sIL-6R is added; this process therefore requires *trans*-signaling (1).

This requirement for sIL-6R was surprising, because IL-6 receptor had been detected in early studies of isolated osteoblasts (14). In later studies, IL-6 *cis*-signaling was reported to induce STAT3 dimerization in undifferentiated calvarial cells

This work was supported by the National Health and Medical Research Council (Australia) through project grant funding (to N. A. S. and T. J. M.). St. Vincent's Institute is supported by the Victorian State Government Operational Infrastructure Support scheme. The authors declare that they have no conflicts of interest with the contents of this article.

This article contains Fig. S1.

[1] This author's contribution was part of an honors year program during which she was supervised at La Trobe University by Associate Professor Brian Grills, who provided essential support for her candidature.

[2] Supported by an Australian Federal Government Endeavor Fellowship.

[3] Supported by an NHMRC Senior Research Fellowship and the SVI Brenda Shanahan Fellowship. To whom correspondence should be addressed: Bone Biology and Disease Unit, St. Vincent's Institute of Medical Research, 9 Princes St., Fitzroy, Victoria 3065, Australia. Tel.: 613-9231-2555; E-mail: nsims@svi.edu.au.

[4] The abbreviations used are: IL, interleukin; IL-6R, IL-6 receptor; sIL-6R, soluble IL-6 receptor; gp130, glycoprotein 130; hIL, human IL; sIL, soluble human IL; CT, computed tomography; ANOVA, analysis of variance; N, newtons; MPa, megapascals; OSM, oncostatin M.

(15). However, gp130 phosphorylation in response to IL-6 was not detected in undifferentiated MC-3T3-E1 cells and only detected in calvarial cells or MG-63 human osteosarcoma cells when soluble IL-6R was added (16, 17). This and the finding that alkaline phosphatase activity was increased by IL-6 only when sIL-6R was added both in MC-3T3-E1 cells (15) and MG-63 cells (17) led to the conclusion that the IL-6R expressed by osteoblasts is nonfunctional. Any effect of IL-6 on the osteoblast lineage was therefore thought to be mediated only by *trans*-signaling through soluble receptor.

These early studies were conducted in undifferentiated calvarial cells, rather than differentiated osteoblasts. Evidence has now accumulated for IL-6 action on differentiated osteoblasts and on the most mature member of the osteoblast lineage, the osteocyte. Differentiated MC-3T3-E1 cells phosphorylate STAT3 in response to IL-6, and this is enhanced with further differentiation (18). Osteocytes express detectable membrane-bound IL-6 receptor (19), suggesting they may be capable of *cis*-signaling. IL-6 is also produced by osteocytes *in vivo* (20) and in the MLO-Y4 osteocyte-like cell line (21). This suggests IL-6 may act in a paracrine or autocrine manner within the osteocyte network.

We sought to determine whether IL-6 *cis*- and *trans*-signaling occurs in osteocytes. Because gp130-binding cytokines stimulate bone formation at least in part through actions on osteocytes (22), we also tested whether IL-6 can stimulate bone formation *in vivo* and used a pharmacological genetic approach to determine whether IL-6 *trans*-signaling is required for normal bone structure. In addition, because osteocytes have been implicated as a source of RANKL that supports osteoclast formation (23, 24), we determined whether osteocytes support osteoclast formation in response to IL-6 *cis*- and *trans*-signaling *in vitro*.

Results

Osteocytes exhibit gene responses to IL-6 cis- and trans-signaling

Primary calvarial osteoblasts differentiated for 21 days to a stage expressing the osteocyte marker sclerostin (25), indicating the presence of osteocytes, showed gene responses to IL-6, without requiring sIL-6R addition.

At 1 h, IL-6 treatment at both 10 and 100 ng/ml led to a significant (>8-fold) increase in mRNA levels of the STAT3 early response gene *Socs3* (Fig. 1*A*). This suggests IL-6 can phosphorylate STAT3 via *cis*-signaling in differentiated osteoblasts. The response was further up-regulated by *trans*-signaling when sIL-6R was added; sIL-6R alone had no effect on *Socs3* expression (Fig. 1*A*).

IL-6 treatment at both 10 and 100 ng/ml also significantly (>4-fold) increased mRNA levels of the STAT3-responsive gene C/EBPδ (*Cebpd*) (Fig. 1*B*). This response was further up-regulated with the addition of sIL-6R, and sIL-6R alone had no effect on *Cebpd* transcript levels (Fig. 1*B*). Because other IL-6 family members have also been reported to suppress sclerostin (25), we investigated whether sclerostin was down-regulated by IL-6 in the presence or absence of sIL-6R. However, although sclerostin mRNA levels were detectable, they were highly variable in untreated primary calvarial cells, and these results were inconclusive (data not shown).

After 6 h of treatment, IL-6 treatment alone of differentiated primary calvarial osteoblasts did not significantly up-regulate RANKL mRNA levels (*Tnfsf11*) (Fig. 1*C*), but with the addition of sIL-6R, *Tnfsf11* mRNA was significantly elevated (Fig. 1*C*), consistent with previous findings that IL-6 does not stimulate osteoclast formation through *cis*-signaling.

Osteocytes phosphorylate STAT3 in response to IL-6 cis- and trans-signaling

We assessed whether the above *cis*- and *trans*-signaling gene responses are associated with STAT3 phosphorylation. Primary calvarial osteoblasts differentiated for 21 days, to a stage when sclerostin is expressed (25), exhibited STAT3 tyrosine phosphorylation in response to treatment with IL-6 alone at very high IL-6 doses (100 ng/ml), indicating a limited *cis*-signaling response. Phosphorylation was detected in response to 10 ng/ml IL-6 if sIL-6R was provided (Fig. 1*D*), indicating *trans*-signaling. This is consistent with previous observations in undifferentiated primary calvarial cells (*i.e.* stromal cells), where STAT3 homodimerization in response to IL-6 was observed, and was augmented when sIL-6R was added (15).

Because the differentiated primary calvarial cells are not a purified cell line, we also tested the effects of IL-6 in the osteocyte cell line Ocy454. In these cells, STAT3 phosphorylation was observed at similar levels whether sIL-6R was provided or not (Fig. 1*E*). This suggests Ocy454 cells respond via both *cis*- and *trans*-signaling. Signaling via *trans*-signaling was also observed with the addition of hyper-IL-6, a fusion protein of IL-6 plus the soluble receptor, capable only of *trans*-signaling (Fig. 1*E*, *far right lanes*). When *Tnfsf11* mRNA levels were assessed in Ocy454 cells treated with IL-6, no response was detected unless sIL-6R was added (Fig. 1*F*). This also indicates that whereas osteocytes can respond to *cis*- and *trans*-signaling, IL-6 only stimulates RANKL via *trans*-signaling.

Osteocytes secrete soluble IL-6 receptor

Soluble IL-6 receptor is generated by cleavage mediated by either ADAM10 or ADAM17. Previous work reported ADAM10 localization in osteoblasts and osteocytes (26), but whether ADAM17 is also expressed by these cells is not known. We interrogated a previous microarray of differentiated primary calvarial osteoblasts (27), and *Adam17* mRNA was detected. By immunohistochemistry, we confirmed positive staining for ADAM17 in osteoblasts and osteocytes in both trabecular (Fig. 2*A*) and cortical (Fig. 2*B*) bone; negative control (IgG) showed no stain (Fig. 2*C*). ADAM17 was also detected in growth plate chondrocytes and was particularly strong in hypertrophic chondrocytes (Fig. 2*A*).

We next assessed sIL-6R production by cultured osteocytes using two osteocyte cell lines. Because all osteocyte cell lines contain both osteocytes and their precursors (osteoblasts), we differentiated the cells to allow sIL-6R production to be assessed as the proportion of osteocytes within the culture increase. We first used differentiated Kusa4b10 cells, which we have previously shown to express sclerostin after differentiation for 21 days, with the increasing presence of osteocytes (25). Increased sclerostin expression at 14 and 21 days was confirmed by quantitative PCR (Fig. 3*A*). IL-6 receptor (*Il6ra*) mRNA levels were also greater after 14 and 21 days of differentiation, reaching levels ~3-fold higher

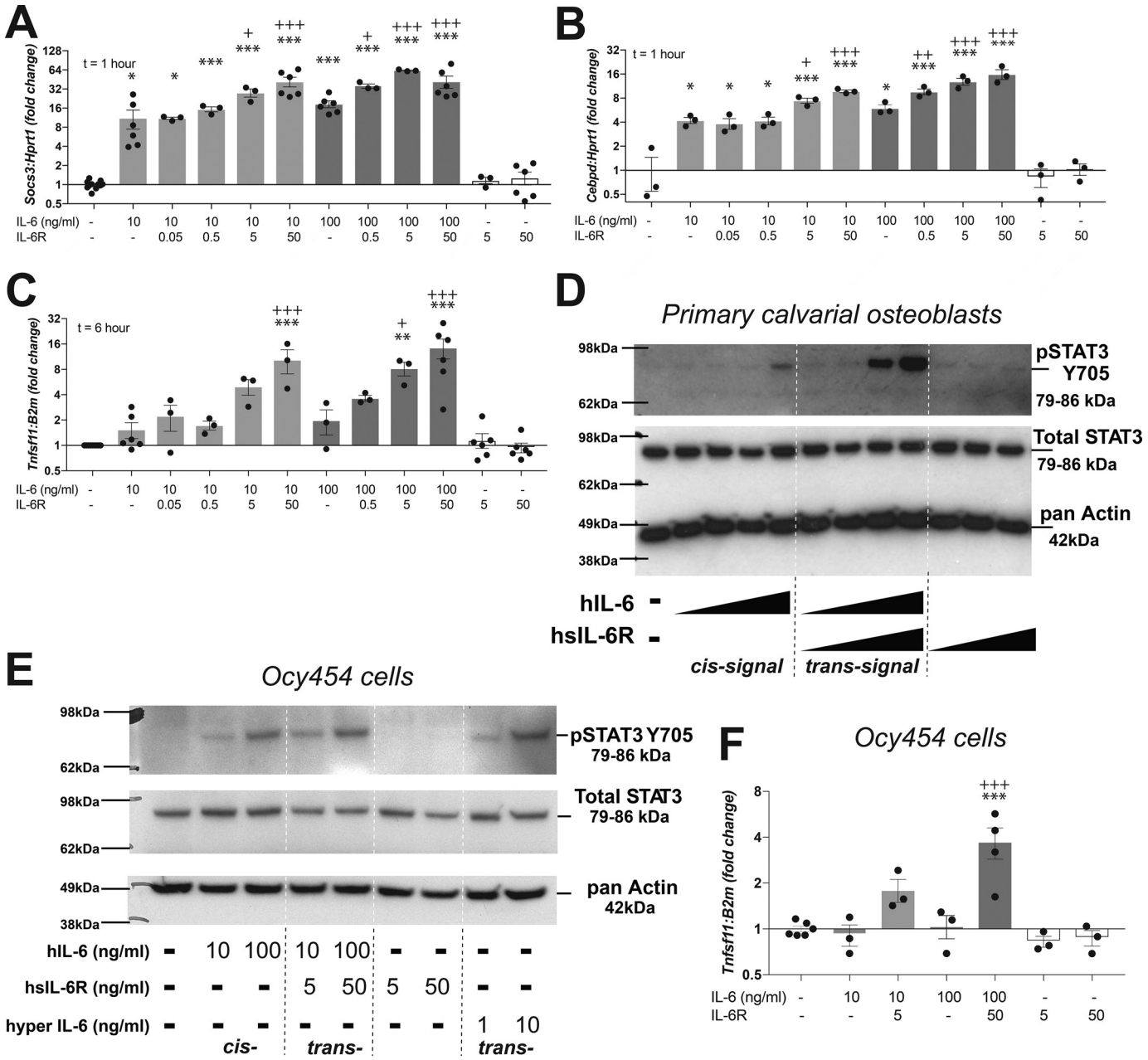

Figure 1. Differentiated osteoblasts and osteocytes respond to IL-6 via both *cis*- and *trans*-signaling. *A–C*, up-regulation of *Socs3* (*A*), C/EBPδ (*Cebpd*) (*B*), and the RANKL gene (*Tnfsf11*) (*C*) in primary calvarial osteoblasts differentiated for 21 days and then stimulated with hIL-6 in the presence or absence of sIL-6R. Data are mean ± S.E. (*error bars*) of 3–6 independent experiments; individual data points shown. *, $p < 0.05$; **, $p < 0.01$; ***, $p < 0.001$ *versus* control. +, $p < 0.05$; ++, $p < 0.01$; +++, $p < 0.001$ *versus* IL-6 at the same concentration without sIL-6R, both by one-way ANOVA and Tukey's post hoc test. *D* and *E*, tyrosine phosphorylation of STAT3(Y705) and total STAT3 levels in differentiated primary calvarial osteoblasts (*D*) and differentiated Ocy454 cells (*E*) treated with hIL-6 at 0.1, 1, 10, and 100 ng/ml (*A*) or 10 and 100 ng/ml (*B*) in the absence or presence of sIL-6R (0.1, 1, 10, and 100 ng/ml in *D* and 5 or 50 ng/ml in *E*). Cells did not respond to sIL-6R alone. Hyper-IL-6, a fusion protein of IL-6 and sIL-6R, also stimulated STAT3 phosphorylation in Ocy454 cells (not tested in primary calvarial osteoblasts). Phosphorylation was assessed 15 min after treatments. Blots are representative of three independent experiments. *F*, up-regulation of *Tnfsf11* in Ocy454 cells, differentiated for 14 days, and then stimulated with hIL-6 in the presence or absence of sIL-6R. Data are mean ± S.E. of 3–6 independent experiments; individual data points shown. ***, $p < 0.001$ *versus* untreated, $^{+++}$, $p < 0.001$ versus IL-6 (100 ng/ml) by one-way ANOVA and Tukey's post hoc test.

than baseline by day 21 (Fig. 3*B*). In addition, sIL-6R was detected at the protein level in conditioned media from these cells at 19 and 21 days of differentiation (Fig. 3*C*), indicating soluble IL-6 receptor secretion by cultured osteocytes.

These findings were confirmed in a second cell line, the Ocy454 cells, which differentiate into osteocytes more rapidly than Kusa4b10 cells (28). In these cells, sclerostin expression was significantly elevated by 14 days after differentiation (Fig. 3*D*). Whereas *Il6ra* mRNA levels were not increased with differentiation (Fig. 3*E*), sIL-6R protein was detected by ELISA at 7, 11, and 14 days of differentiation but not detected earlier (Fig. 3*F*), again confirming soluble IL-6 receptor secretion by osteocytes in culture.

IL-6 stimulates bone formation via trans- but not cis-signaling

Oncostatin M, LIF, and cardiotrophin 1 have all been shown to stimulate bone formation *in vivo* by the calvarial injection model (25, 29, 30), but this ability has not been tested for IL-6. We compared IL-6 treatment alone (*cis*) with IL-6 plus soluble

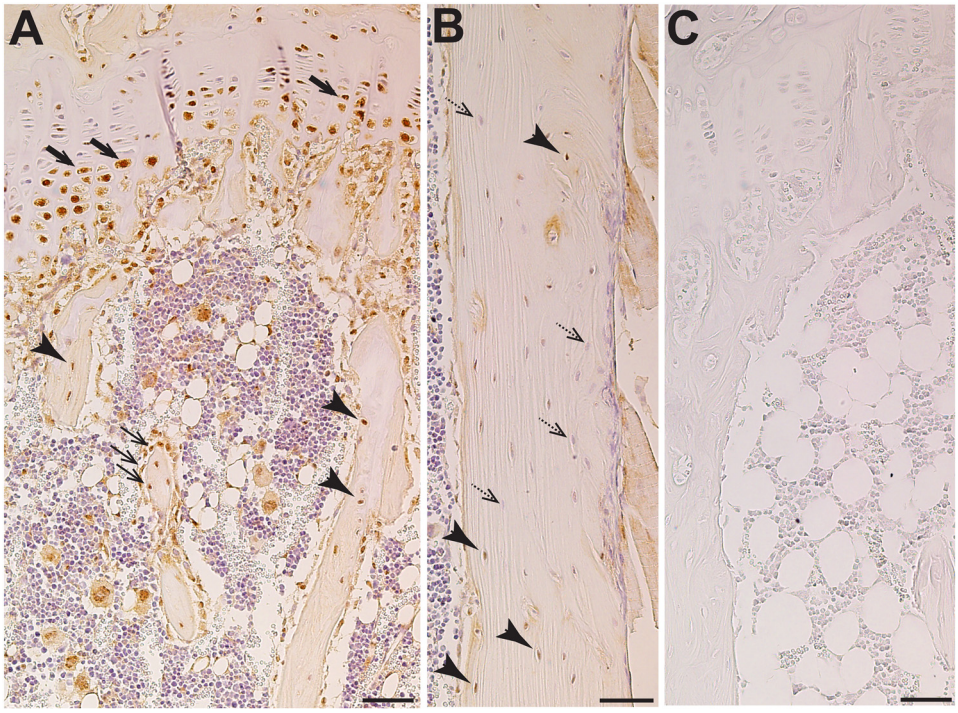

Figure 2. Immunohistochemical localization of ADAM17 in murine bone (12-week-old female C57BL/6). *A*, abundant staining in prehypertrophic and hypertrophic growth plate chondrocytes (*thick arrow*), osteoblasts (*thin arrows*), and all osteocytes (*arrowheads*) in trabecular bone as well as adipocytes and megakaryocytes in the bone marrow. *B*, varied levels of staining in osteocytes in cortical bone; positively stained osteocytes (*arrowheads*) and negatively stained osteocytes (*dashed arrows*) are found both near the bone surface and deeply embedded in the bone. *C*, IgG control. *Scale bar*, 50 μm.

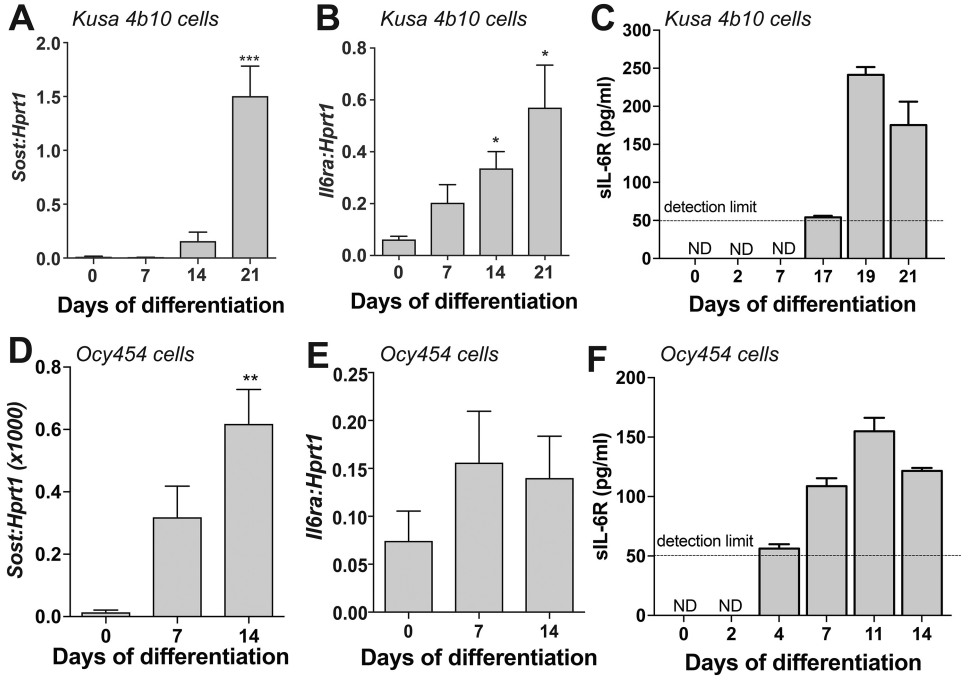

Figure 3. Release of soluble IL-6R by osteocytes *in vitro*. Shown are sclerostin (*Sost*; *A* and *D*) and IL-6 receptor (*Il6ra*; *B* and *E*) mRNA levels and sIL-6R protein levels (*C* and *F*) in cell lysates and conditioned media from differentiating Ocy454 cells (*A–C*) and Kusa4b10 cells (*D–F*). Data are the mean ± S.E. (*error bars*) from three independent preparations. *, $p < 0.05$, **, $p < 0.01$, ***, $p < 0.001$ *versus* undifferentiated cells by one-way ANOVA with Tukey post hoc test; *C* and *F* do not contain statistics because levels were undetectable at day 0.

IL-6R (*cis* plus *trans*). We also tested hyper-IL-6, a fusion protein of IL-6 and sIL-6R, capable only of *trans*-signaling (31). OSM was used as a positive control.

Surprisingly, although IL-6 induced STAT3 phosphorylation and both *Socs3* and *Cebpd* transcription *in vitro* without requiring sIL-6R, five daily injections of IL-6 (Fig. 4*A*) did not increase calvarial thickness *in vivo* (Fig. 4*B*). However, if soluble IL-6R was provided, calvarial thickness was significantly increased (Fig. 4*B*), suggesting that *trans*- but not *cis*-signaling of IL-6 promotes bone formation. To confirm the

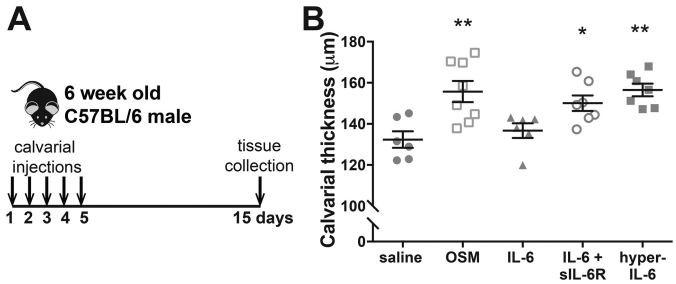

Figure 4. IL-6 treatment stimulates bone formation *in vivo* but requires the addition of sIL-6R. *A*, *schematic diagram*. *B*, calvarial thickness in 6-week-old male C57BL/6 mice with vehicle (saline), hIL-6 alone (0.2 μg/day), hIL-6 (0.2 μg/day) with sIL-6rα (0.1 μg/day), hyper-IL-6 (0.2 μg/day), or murine OSM (0.2 μg/day) by subcutaneous calvarial injections. Data are shown as individual data points for each animal with mean ± S.E. (*error bars*); *, $p < 0.01$, $p < 0.001$ *versus* vehicle by one-way ANOVA with Sidak post hoc test.

effect of IL-6 *trans*-signaling on bone formation, we also used the designer cytokine hyper-IL-6, which is capable of activating only *trans*-signaling. Hyper-IL-6 also increased calvarial thickness. This confirms that IL-6 *trans*- but not *cis*-signaling stimulates bone formation, at least at pharmacological doses. Both approaches to stimulate *trans*-signaling increased calvarial thickness to a similar extent as the positive control, oncostatin M, previously reported to promote bone formation (25). This suggests IL-6, like other members of the same cytokine superfamily, can promote bone formation, but requires soluble IL-6R (*i.e.* through *trans*-signaling).

IL-6 stimulates osteoclastogenesis via trans-signaling in osteoblasts but not via osteocytes

We next assessed whether osteocytes might support osteoclast formation in response to IL-6. We conducted side-by-side analyses of osteoclast formation in the presence of either undifferentiated primary calvarial osteoblasts as the supportive cell type (Fig. 5, *A–F*) or Ocy454 cells as support (Fig. 5, *G–L*).

As reported previously, primary calvarial osteoblasts supported osteoclast differentiation in response to IL-6 only when soluble IL-6R was added (Fig. 5, *A* and *B*). In addition, and again as previously reported (1), they also supported osteoclast differentiation in response to oncostatin M (Fig. 5, *A* and *C*) and 1,25-dihydroxyvitamin D_3/prostaglandin E_2 (Fig. 5, *A* and *D*).

In contrast, when Ocy454 cells were used, osteoclast formation was not observed beyond the binucleate stage with these stimuli (Fig. 5*G*). IL-6, only with sIL-6R addition, induced TRAP+ mononuclear osteoclast precursor formation but did not induce formation of TRAP+ cells with any more than two nuclei (Fig. 5, *G* and *H*). The number of mononuclear precursors and binucleate TRAP+ cells formed was far lower than the number formed when primary calvarial osteoblasts were used (Fig. 5, *A* and *B*). Similar results were observed with oncostatin M (Fig. 5, *B* and *H*) and 1,25-dihydroxyvitamin D_3/prostaglandin E_2 (Fig. 5, *D* and *J*). No osteoclasts or TRAP+ mononuclear cells were formed when IL-6 or sIL-6R alone were supplied to co-cultures containing either undifferentiated primary osteoblasts or Ocy454 cells (Fig. 5, *E*, *F*, *K*, and *L*).

High circulating levels of soluble gp130-Fc limit bone growth and impair bone strength

Because both bone formation and osteoclast formation are stimulated by IL-6 *trans*-signaling, but not *cis*-signaling, we next determined whether specific systemic pharmacological inhibition of IL-6 *trans*-signaling would modify bone structure. To do this, we assessed the phenotype of the PEPCK-soluble gp130 (sgp130) mouse. In this model, IL-6 *trans*-signaling is inhibited systemically by liver-targeted overexpression of the *trans*-signaling inhibitor sgp130-Fc, which is then detected in the circulation (32).

In our first study, we observed highly divergent results, with some mice exhibiting very low bone mass and others showing normal structure. Earlier work (32) reported lower circulating sgp130-Fc levels in PEPCK-sgp130 hemizygotes compared with homozygotes. Because our genotyping could not distinguish between hemizygotes and homozygotes, we assessed serum levels of human sgp130 by ELISA and segregated mice into sgp130-Fc^{high} (>10 μg/ml) and $sgp130^{low}$ (<10 μg/ml) based on the earlier work (32).

Male sgp130-Fc^{high} mice had low body weight and femur length compared with nontransgenic controls (Fig. 6, *B* and *C*); this was not statistically significant in the smaller cohort of female mice. Male sgp130-Fc^{low} mice did not exhibit a significant change in body weight or femur length (Fig. 6, *B* and *C*).

Both male and female sgp130-Fc^{high} mice exhibited significantly lower trabecular bone volume (Fig. 6, *D* and *E*), trabecular number (Fig. 6*F*) and trabecular thickness (Fig. 6*G*) than controls. In female sgp130-Fc^{high} mice, trabecular bone volume was approximately half that of controls, whereas in males, it was reduced by ~25%. Sgp130-Fc^{low} mice did not exhibit a significant reduction in trabecular bone volume (Fig. 6, *E–H*).

These mice also showed impaired growth. Both male and female gp130-Fc^{high} mice had narrower femora in both the mediolateral and anteroposterior dimensions (Fig. 7, *A* and *B*). This was confirmed by microcomputed tomography (micro-CT), which detected a smaller periosteal perimeter (Fig. 7*C*), narrower cortical bone (Fig. 7*D*), lower moment of inertia (Fig. 7*E*), and, in males only, smaller marrow area (Fig. 7*F*).

Mechanical testing indicated a reduction in bone strength; this was not limited to gp130-Fc^{high} mice. In femora from male gp130-Fc^{high} mice, we detected significantly lower ultimate force and failure force, and higher ultimate stress, failure stress, and yield stress, but other parameters were not significantly modified (Table 1). In femora from female gp130-Fc^{high} mice, the ultimate force before breaking was reduced by almost a third (Table 1), and the bones were less able to deform (Table 1). Female gp130-Fc^{low} mice also exhibited significantly lower ultimate and yield forces (Table 1). After correction for bone shape, there was no defect in material strength detected in female gp130-Fc^{low} mice (Table 1), but female gp130-Fc^{high} mice exhibited reduced ultimate, yield, and post-yield strains and significantly lower material toughness and elastic modulus (Table 1). These data indicate that high pharmacological levels of sgp130-Fc restrict growth, including bone growth, and limit accrual of bone mass and strength.

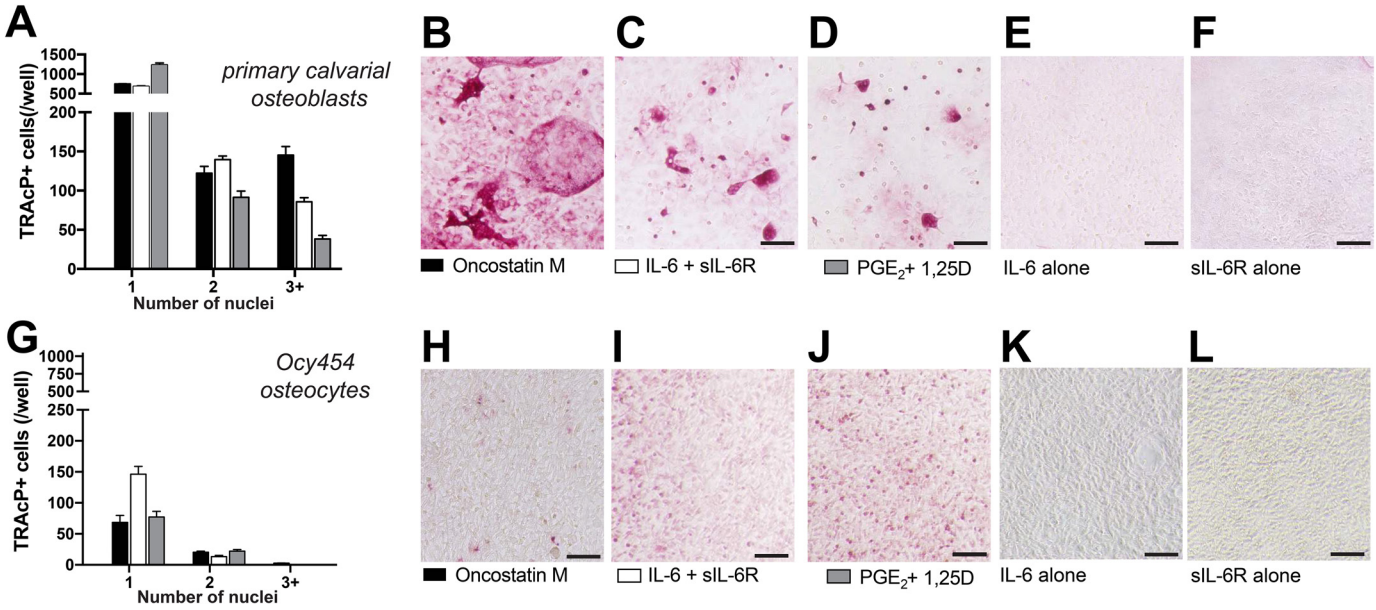

Figure 5. Osteocytes do not fully support osteoclast formation in response to IL-6 or other stimuli. Osteoclast and osteoclast precursor formation (TRAcP+ cells) were measured in co-culture assays of bone marrow macrophages with either primary calvarial osteoblasts (*A–F*) or Ocy454 osteocytes (*G–L*). TRAcP+ cells were counted in three categories: single nuclei (precursors), two nuclei (binucleated cells), and three or more nuclei (osteoclasts). Stimuli were IL-6 alone (40 ng/ml), IL-6 (40 ng/ml) plus soluble IL-6 receptor (100 ng/ml), sIL-6R alone (100 ng/ml), oncostatin M (50 ng/ml), or prostaglandin E_2 plus 1,25-dihydroxyvitamin D_3 (both at 10 nM) for 7 days. No TRAcP-positive cells were formed in cultures supplied with IL-6 or sIL-6R alone; only representative images are shown from these treatments. Data are the mean ± S.E. (*error bars*) from three independent experiments, each performed in triplicate. Images are representative, showing TRAcP+ cells (*red stain*). *Scale bars*, 100 μm.

Hemizygous mice overexpressing soluble gp130-Fc have no significant bone phenotype

Because there was large data variability in the sgp130-Fc^{low} group, we were concerned about misclassification on the basis of sgp130 levels (note particularly, two male mice in the sgp130-Fc^{low} group with bone mass and body weight consistently within the range of the sgp130-Fc^{high} group). We then carried out a second experiment, where we bred and assessed hemizygous sgp130-Fc mice, to determine the effects of only low levels of sgp130-Fc throughout life. In all but one hemizygous mouse, sgp130-Fc levels were <10 μg/ml (Table 2 and Fig. S1).

When the hemizygous mice were assessed by micro-CT, no significant modifications in trabecular structure, longitudinal bone growth, or cortical bone structure were observed (Table 2). This suggests consistently low doses of sgp130-Fc may avoid the side effects seen with high sgp130-Fc levels on bone growth and bone mass.

Discussion

We report four novel findings. (i) Osteocytes in cell culture secrete soluble IL-6R, and like osteoblasts, they respond to IL-6 with STAT3 phosphorylation and changes in gene expression through both *cis*- and *trans*-signaling; however, (ii) IL-6 stimulates bone formation *in vivo* only through *trans*-signaling. (iii) In contrast to osteoblasts, osteocytes do not support osteoclast formation in response to IL-6 via either *cis*- or *trans*-signaling *in vitro*. (iv) Despite the ability of IL-6 to promote both bone formation and osteoclastogenesis via *trans*-signaling, pharmacological suppression of IL-6 *trans*-signaling did not result in a significant bone phenotype unless very high circulating levels of sgp130-Fc were provided, in which case bone growth and strength were compromised. These actions of IL-6 are illustrated in Fig. 8.

As cultured osteoblasts differentiated into osteocytes, they gained the capacity to release sIL-6R into their local environment. This suggests osteocyte-derived sIL-6R may support IL-6 action in osteoblast lineage cells to stimulate osteoclast formation or bone formation. Soluble IL-6R is generated by ectodomain shedding by proteases, particularly the metalloproteinase ADAM10 and its close homolog ADAM17 (33–35). Release of sIL-6R by osteocytes is consistent with localization of ADAM10 (26) and ADAM17 (this work) in osteocytes. ADAM17 was also strongly detected in hypertrophic chondrocytes, consistent with its reported role in promoting chondrocyte hypertrophy (36). This suggests hypertrophic chondrocytes may also provide sIL-6R to osteoblasts and osteocytes; this remains to be investigated. ADAM17 expression by osteocytes not only has relevance for sIL-6R production, but it may also regulate receptor activities in osteocytes, because ADAM17 also act as a sheddase for chemokine and growth factor receptors and ligands (37).

Our observation that IL-6 *trans*-signaling stimulates bone formation *in vivo* is consistent with early *in vitro* studies showing IL-6 could stimulate alkaline phosphatase activity of stromal cell cultures (15). The ability of IL-6 to increase calvarial thickness indicates it shares the ability previously noted for other IL-6 family cytokines, such as LIF, oncostatin M (OSM), and CT-1, to promote bone formation in this model (25, 29, 30). Surprisingly, although IL-6 could increase mRNA levels of the STAT3-responsive genes *Socs3* and *Cebpd* through *cis*-signaling, calvarial thickness was increased only in response to *trans*-signaling, either by the addition of sIL-6R or through the use of

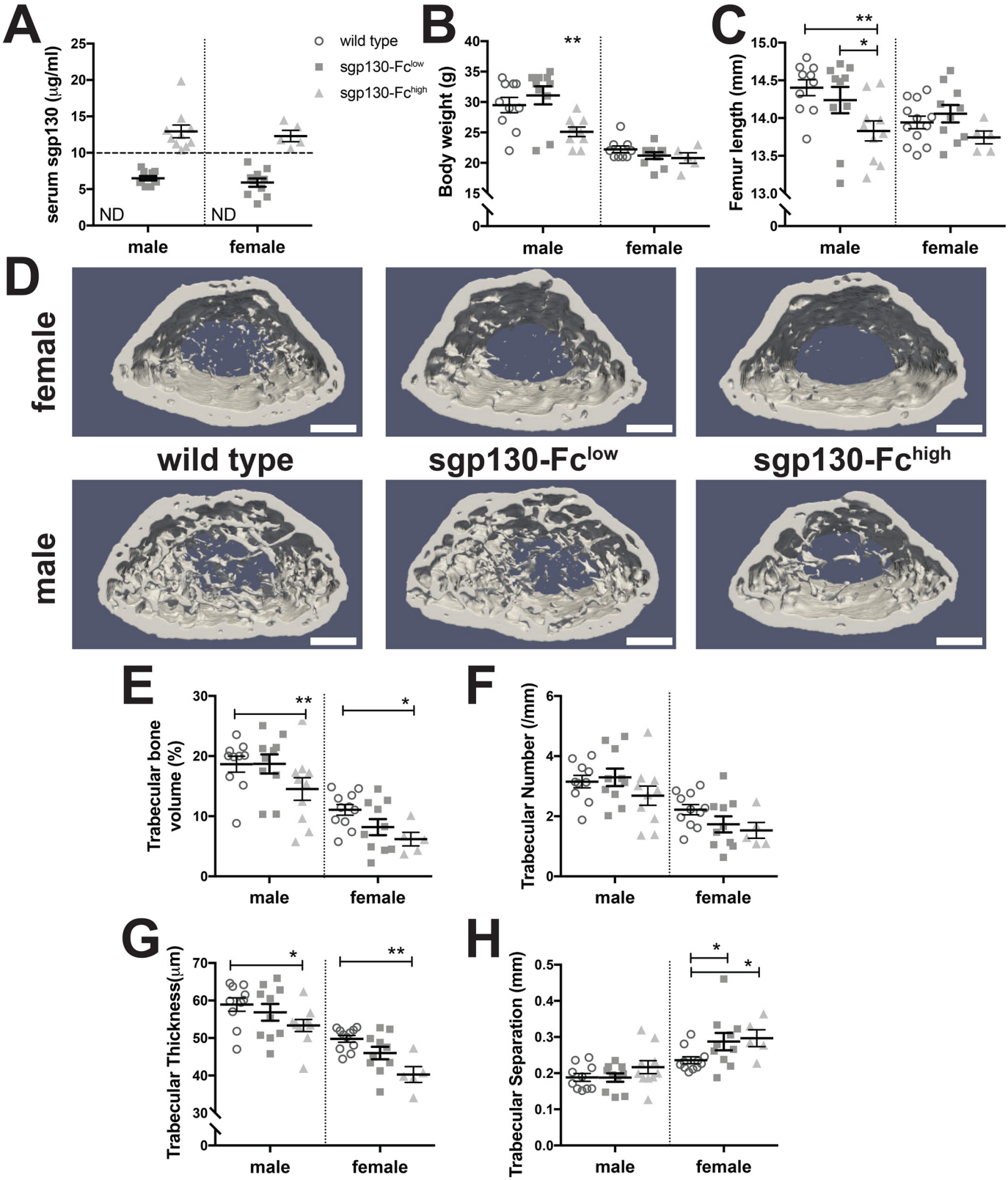

Figure 6. Male and female PEPCK-sgp130-Fc mice demonstrate impaired growth and low trabecular bone mass at high levels of sgp130-Fc. *A*, serum human gp130 levels at 12 weeks of age used to segregate mice into sgp130-Fc^{low} (gp130 $<$ 10 μg/ml) and sgp130-Fc^{high} (gp130 $>$ 10 μg/ml) groups. Shown are total body weight (*B*) and femoral length (*C*) at 12 weeks of age in male and female sgp130-Fc^{low} and sgp130-Fc^{high} mice. *D*, representative images of the trabecular region, showing reduced trabecular bone mass in both male and female sgp130-Fc^{high} mice. *Scale bar*, 500 μm. *E–G*, quantification of trabecular structure in 12-week-old male and female sgp130-Fc^{low} and sgp130-Fc^{high} mice. Data are shown as individual data points and means with S.E. (*error bars*) for each group; n = 5–12/group. *, $p < 0.05$; **, $p < 0.01$ for comparison with WT mice of the same sex and age by two-way ANOVA.

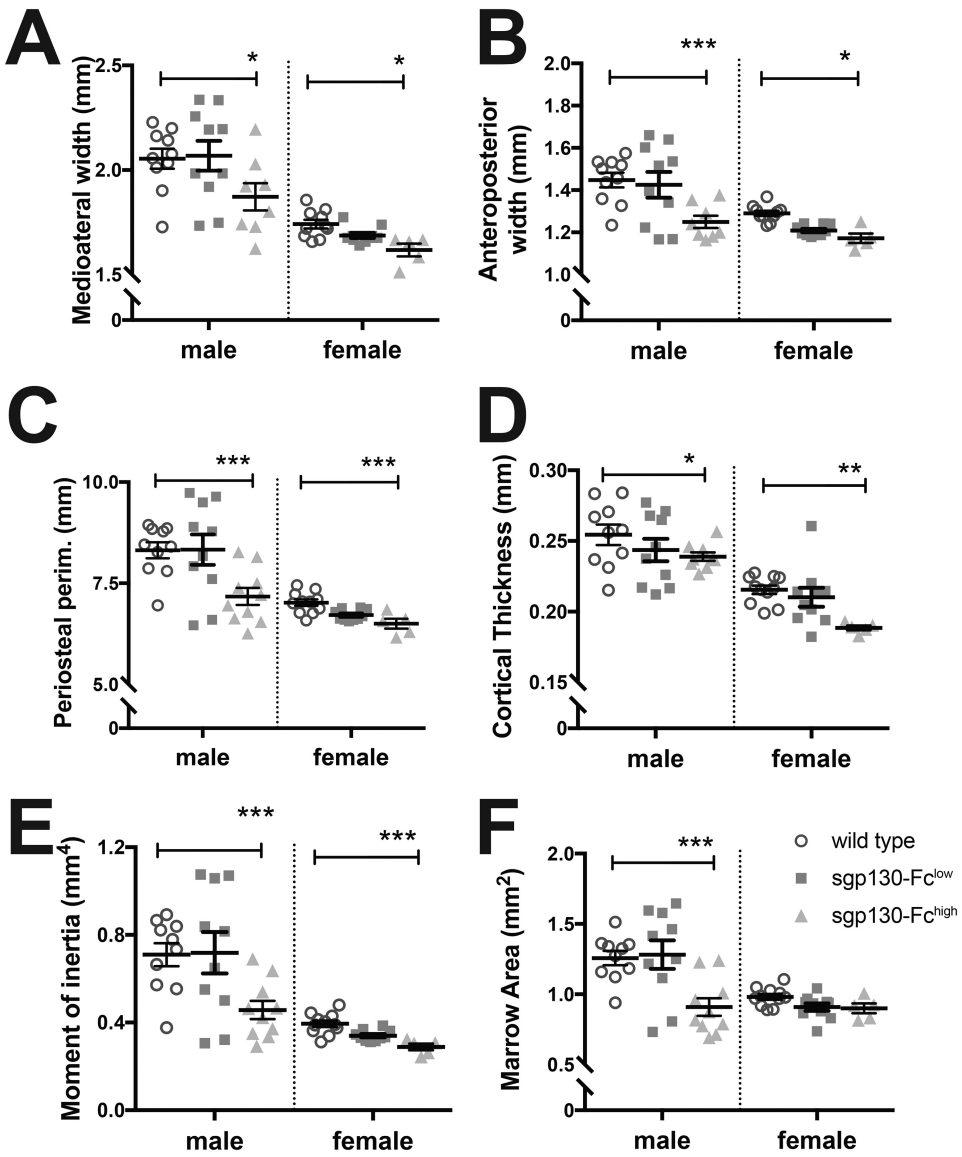

Figure 7. Male and female PEPCK-sgp130-Fc mice have narrower cortical bone at high levels of sgp130-Fc. Caliper measurements of mid-diaphyseal femoral mediolateral and anteroposterior widths (*A* and *B*), and quantitative micro-CT data for femoral periosteal perimeter, cortical thickness, moment of inertia, and marrow area (*C–F*) in 12-week-old male and female sgp130-Fc^{low} and sgp130-Fc^{high} mice; data shown as individual data points and means with S.E. (*error bars*) for each group; $n = 5–12$/group. *, $p < 0.05$; **, $p < 0.01$; ***, $p < 0.001$ for comparison with WT mice of the same sex and age by two-way ANOVA.

hyper-IL-6. Physiological sIL-6R levels, provided either locally by osteocytes or through the blood stream (38), may be insufficient to support pharmacological IL-6 doses in stimulating bone formation. Another question raised is whether sIL-6R produced by osteocytes can gain access to osteoblast precursors near the bone surface; sIL-6R is sufficiently small (50–55 kDa) to pass through the osteocyte lacunocanalicular network by convective transport (39). Bone formation may be stimulated by endogenous IL-6 when sIL-6R levels are elevated locally in response to as yet unknown stimuli or when sIL-6R levels are elevated in the bloodstream. One likely example is estrogen deficiency (40). Our recent report showing reduced bone formation in ovariectomized mice treated with an antibody targeted against IL-6 *trans*-signaling (41) provides evidence for this and suggests IL-6 *trans*-signaling may promote bone formation in such conditions. IL-6 *trans*-signaling may also promote bone formation during growth, as suggested by the narrow cortical bone (3) and impaired bone formation on the periosteal surface (42, 43) in IL-6 null mice.

Osteocytic RANKL expression was identified *in situ* in 1999 (44), and mild osteopetrosis in mice with RANKL deletion targeted to osteocytes has been interpreted as evidence for osteocytes as the major source of RANKL within the skeleton (23, 24). At the time, questions were raised about how RANKL produced by osteocytes could induce osteoclast formation, because osteocytes are deeply embedded in the bone, and direct cell–cell contact between stromal cells and osteoclast precursors is required for factors such as IL-6 (with sIL-6R) to stimulate osteoclastogenesis *in vitro* (45). Furthermore, although soluble RANKL can be shed by the actions of, among others, ADAM10 and ADAM17 (46), RANKL shedding inhibits osteoclastogenesis by limiting the amount of available membrane-bound

Table 1

Three-point bending tests of male and female sgp130-Fc^{low} and sgp130-Fc^{high} femora

Data from 12-week-old male and female PEPCK-sgp130-Fc mice (hemizygotes) are shown as mean ± S.E. No significant differences associated with the PEPCK-sgp130-Fc genotype were detected in any parameters, assessed by two-way ANOVA. Sex differences were observed in all parameters in both wild type (WT) and PEPCK-sgp130-Fc mice and are not shown. Genotype effects shown as: *, $p < 0.05$; **, $p < 0.01$; ***, $p < 0.001$ *versus* sex-matched WT.

	Male			Female		
	WT ($n = 9$)	sgp130-Fc^{low} ($n = 6$)	sgp130-Fc^{high} ($n = 7$)	WT ($n = 10$)	sgp130-Fc^{low} ($n = 10$)	sgp130-Fc^{high} ($n = 4$)
Structural strength						
Ultimate force (N)	24.06 ± 1.55	27.54 ± 1.67	18.79 ± 1.19**	14.75 ± 0.51	12.38 ± 0.38**	10.68 ± 0.18***
Ultimate deformation (mm)	0.556 ± 0.062	0.531 ± 0.048	0.580 ± 0.059	0.474 ± 0.063	0.442 ± 0.028	0.359 ± 0.032*
Stiffness (N/mm)	77.5 ± 8.9	82.8 ± 8.1	56.3 ± 7.1	43.6 ± 3.9	39.2 ± 3.4	38.2 ± 2.0
Yield force (N)	20.56 ± 1.59	25.15 ± 0.92	17.95 ± 1.51	13.64 ± 0.62	11.52 ± 0.38*	7.90 ± 0.67***
Yield deformation (mm)	0.469 ± 0.071	0.488 ± 0.058	0.539 ± 0.073	0.415 ± 0.035	0.384 ± 0.040	0.221 ± 0.015*
Energy to failure (mJ)	6.52 ± 0.65	7.34 ± 0.78	4.89 ± 0.48	6.91 ± 0.61	5.66 ± 0.30	7.12 ± 1.24
Failure force (N)	23.94 ± 1.55	26.97 ± 2.07	18.43 ± 1.10*	10.63 ± 0.56	8.71 ± 0.85	6.17 ± 1.62*
Material strength						
Ultimate stress (MPa)	35.67 ± 3.44	38.86 ± 9.16	56.15 ± 8.74*	51.55 ± 2.12	54.31 ± 2.14	60.89 ± 6.7
Ultimate strain (%)	0.060 ± 0.006	0.059 ± 0.006	0.053 ± 0.005	0.037 ± 0.002	0.032 ± 0.002	0.025 ± 0.001**
Yield stress (%)	29.4 ± 1.4	36.5 ± 9.2	53.7 ± 9.0*	47.8 ± 2.7	50.7 ± 2.4	44.8 ± 5.3
Yield strain (%)	0.051 ± 0.007	0.053 ± 0.007	0.049 ± 0.006	0.032 ± 0.003	0.028 ± 0.003	0.016 ± 0.001**
Post-yield strain %)	0.010 ± 0.002	0.011 ± 0.004	0.005 ± 0.002	0.023 ± 0.004	0.024 ± 0.004	0.059 ± 0.018**
Elastic modulus (MPa)	1059 ± 160	1237 ± 428	1891 ± 415	1953 ± 156	2325 ± 155	3138 ± 441**
Toughness (mJ/mm^3)	1.10 ± 0.12	1.14 ± 0.17	1.27 ± 0.16	1.83 ± 0.11	1.78 ± 0.08	2.73 ± 0.29**
Failure stress (MPa)	35.5 ± 3.5	37.3 ± 9.3	55.1 ± 8.7*	37.7 ± 3.1	38.3 ± 3.8	37.7 ± 12.86

Table 2

Hemizygous PEPCK-sgp130-Fc mice have normal trabecular and cortical bone mass

Data from 12-week-old male and female PEPCK-sgp130-Fc mice (hemizygotes) are shown as mean ± S.E. No significant differences associated with the PEPCK-sgp130-Fc genotype were detected in any parameters, assessed by two-way ANOVA. Sex differences were observed in all parameters in both control and PEPCK-sgp130-Fc mice: *, $p < 0.05$; **, $p < 0.01$; ***, $p < 0.001$ *versus* female control; $^+$, $p < 0.001$ *versus* sex-matched control.

	Female		Male	
	Control ($n = 8$)	PEPCK-sgp130-Fc ($n = 8$)	Control ($n = 8$)	PEPCK-sgp130-Fc ($n = 7$)
Serum human gp130 (μg/ml)	Undetectable	4.756 ± 1.34$^+$	Undetectable	2.410 ± 0.37$^+$
Trabecular bone				
Trabecular bone volume (%)	8.14 ± 0.61	7.01 ± 0.92	19.76 ± 1.44***	20.55 ± 1.80***
Trabecular thickness (μm)	45.1 ± 0.6	43.6 ± 0.9	53.4 ± 1.1***	54.5 ± 1.2***
Trabecular number (/mm)	1.80 ± 0.12	1.60 ± 0.18	3.68 ± 0.21***	3.74 ± 0.26***
Trabecular separation (μm)	248.6 ± 4.8	279.5 ± 16.6	167.9 ± 4.8***	164.4 ± 9.6***
Bone size and shape				
Femoral length (mm)	14.18 ± 0.06	14.10 ± 0.13	14.33 ± 0.16	14.38 ± 0.10
Cortical thickness (μm)	216 ± 4	213 ± 4	234 ± 8*	245 ± 9**
Periosteal circumference (μm)	6.92 ± 0.09	6.87 ± 0.06	8.08 ± 0.36**	7.90 ± 0.27**
Marrow area (mm^2)	0.95 ± 0.03	0.94 ± 0.01	1.22 ± 0.09**	1.13 ± 0.06*
Cortical area (mm^2)	0.84 ± 0.02	0.82 ± 0.02	1.05 ± 0.08*	1.07 ± 0.06**
Mean polar moment of inertia (mm^4)	0.38 ± 0.01	0.36 ± 0.02	0.64 ± 0.09**	0.61 ± 0.07*

RANKL (47). Although RANKL was induced by IL-6 *trans*-signaling in Ocy454 cells, this was insufficient to induce osteoclast formation *in vitro*. Only binucleated TRAP+ cells were formed. This was not specific to IL-6 *trans*-signaling; in the present work, we also observed only binucleated TRAP+ cells in co-cultures stimulated with other robust osteoclast stimuli, oncostatin M, and 1,25-dihydroxyvitamin D_3 combined with prostaglandin E_2. This is similar to our earlier work using highly purified osteocytes derived by FACS from mice with GFP-labeled osteocytes, which supported only the formation of binucleated TRAP+ cells when stimulated with 1,25-dihydroxyvitamin D_3 combined with prostaglandin $E_{2,}$ (48). Our data again indicate that osteocytes, even in direct contact with osteoclast precursors, and even when stimulated to produce RANKL, do not fully support osteoclast formation.

Because IL-6 *trans*-signaling stimulated both bone formation and osteoclastogenesis (although not through osteocytes), we used transgenic mice expressing circulating sgp130-Fc (32) to determine whether *trans*-signaling is essential for bone growth and remodeling. Although monomeric sgp130 can inhibit signaling by all IL-6 family cytokines (including LIF, CT-1, OSM, and CNTF) (49, 50), dimeric sgp130-Fc, which is expressed in these mice, was designed as a pharmacological agent to specifically block IL-6 *trans*-signaling (51). When hemizygous sgp130-Fc mice were studied, there was no significant alteration in bone mass in either female or male mice, despite inhibition of IL-6 *trans*-signaling throughout life. However, when sgp130-Fc levels were high, in male and female sgp130-Fc^{high} mice, there were major effects on bone growth, mass, and strength. sgp130-Fc is currently in clinical trials for chronic inflammatory conditions (52), including colitis and rheumatoid arthritis, conditions both associated with low bone mass. In light of this, side effects on the skeleton should be considered, and doses sufficiently low to prevent bone loss might need to be established.

The low bone mass and strength observed in male and female sgp130-Fc^{high} mice contrasts strongly with the mild phenotype in global IL-6 null mice (3, 42) and implies that high sgp130-Fc may suppress a broader range of bone-active cytokines. Indeed, high sgp130-Fc levels inhibit LIF and OSM signaling in BaF3

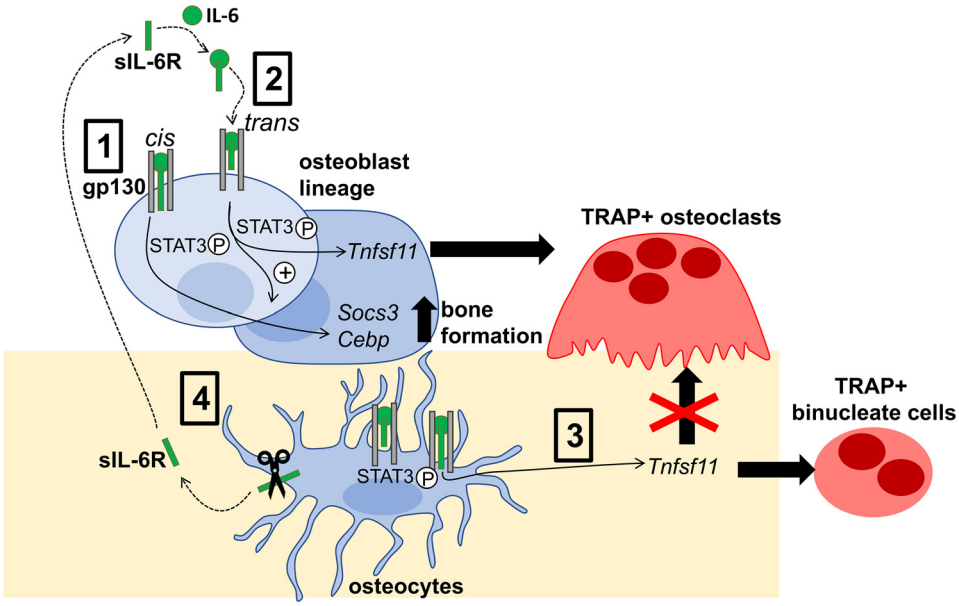

Figure 8. *Schematic diagram* of IL-6 action in the osteoblast lineage. IL-6 signals through gp130 in the osteoblast lineage (osteoblast precursors, osteoblasts, and osteocytes) via *cis*-signaling, where it binds a membrane-bound IL-6 receptor and a gp130 homodimer (*1*), or *trans*-signaling, where it binds sIL-6R, which subsequently interacts with a gp130 homodimer (*2*). *Cis*-signaling promotes STAT3 phosphorylation and increases *Socs3* and *Cebpb* mRNA levels. *Trans*-signaling further promotes STAT3 phosphorylation and further increases both *Socs3* and *Cebpb* mRNA levels, thereby promoting bone formation. *Trans*-signaling also increases *Tnfsf11* mRNA levels in both osteoblasts and osteocytes (*3*). Increased RANKL production by osteoblast precursors and osteoblasts supports formation of tartrate-resistant acid phosphatase–positive multinucleated osteoclasts. In contrast, increased RANKL production by osteocytes is not capable of supporting osteoclast formation and only supports formation of TRAP+ binucleate cells (*4*). Osteocytes also release sIL-6R into their local environment, likely through the actions of ADAM10 and ADAM17 sheddases, which are both expressed by osteocytes.

cells *in vitro* (49). Because OSMR null mice do not exhibit low bone mass or reduced growth (25), but adult LIF null mice exhibit impaired bone growth and low trabecular bone volume (53), we suggest the sgp130-Fc^{high} bone phenotype results, at least in part, from impaired LIF signaling.

To summarize, this study shows that although IL-6R is released by osteocytes, and IL-6 can signal in both differentiated osteoblasts and osteocytes without addition of exogenous sIL-6R, the ability of IL-6 to promote bone formation requires exogenous sIL-6R. Furthermore, although RANKL production is stimulated in osteocytes in response to IL-6, these cells are not capable of supporting osteoclastogenesis. Finally, whereas IL-6 *trans*-signaling promotes both osteoclast formation and bone formation, blockade with sgp130-Fc does not modify bone structure, unless very high levels are used. We conclude that long-term use of *trans*-signaling inhibitors, such as sgp130-Fc, in chronic inflammatory conditions is unlikely to have detrimental effects on the skeleton but suggest this should be monitored in future studies.

Experimental procedures

Cell culture

Three cell culture models of osteoblasts and osteocytes were used. Primary calvarial osteoblasts were generated from 0–2-day-old C57BL/6 mice, and, as indicated in specific experiments, differentiated until osteocytes were present in the culture, as described previously (54). Ocy454 cells, a murine osteocyte cell line, was obtained from Dr. Paola Divieti-Pajevic and have been described previously (29). Kusa4b10 cells (56), a murine bipotential cell line that can differentiate through to osteocyte gene expression (25), was also used. To promote osteoblast/osteocyte differentiation, all of these cell types were differentiated in Eagles α-minimum essential medium + 15% heat-inactivated fetal bovine serum (JRH Biosciences, Melbourne, batch 379) + 50 μg/ml ascorbate (Sigma) for the times indicated in the figure legends.

To compare the ability of osteoblasts and osteocytes to support osteoclast formation, co-cultures were carried out according to established methods (57) using either undifferentiated primary calvarial osteoblasts or Ocy454 cells as supporting cells. Briefly, bone marrow macrophages from C57BL/6 mice (10^5 cells/well) were added to Ocy454 cells or primary calvarial osteoblasts (each at 2×10^4 cells/well of a 48-well plate). Osteoclast formation was induced by the addition of IL-6 alone (40 ng/ml), IL-6 (40 ng/ml) plus soluble IL-6 receptor (100 ng/ml), oncostatin M (50 ng/ml), or prostaglandin E_2 plus 1,25-dihydroxyvitamin D_3 (both at 10 mM) for 7 days. Osteoclast formation was assessed by TRAP staining, and mononuclear TRAP+ cells, binucleated TRAP+ cells, and TRAP+ cells with more than two nuclei were counted.

ELISA and quantitative real-time PCR

RNA extraction was performed using TRIzol extraction and precipitation with chloroform and isopropyl alcohol as described previously (30). Extracted RNA was then treated with DNase (Ambion Turbo DNA-free Kit (Ambion Inc., Waltham, MA). RNA concentration was measured using a Nanodrop ND-1000 spectrophotometer (Analytical Technologies). cDNA was synthesized by reverse transcription using the AffinityScript QPCR cDNA Synthesis Kit (Agilent

Technologies, Santa Clara, CA), according to the manufacturer's instructions on a Biometra T3000 Thermocycler (Biometra GmbH, Göttingen, Germany). cDNA was diluted 1:5 to 1:10, and quantitative real-time PCR was performed using intercalating dye, SYBR Green Brilliant II (Life Technologies, Inc.) on a Stratagene Mx3000P (Agilent Technologies) quantitative PCR machine (Invitrogen, Waltham, MA). Samples were dispensed into an optically clear 96-well plate (Thermo Scientific, Waltham, MA; 4Titude catalog no. 4ti-0750) and run on a Stratagene Mx3000P (Agilent Technologies) with two-step cycling conditions (95 °C for 10 min; 95 °C for 30 s, 60 °C for 1 min) for 40 cycles, followed by a dissociation step (95 °C for 1 min, 55 °C for 30 s, 95 °C for 30 s). Post-run samples were analyzed using Stratagene software MxPro and reported using linear Δ threshold cycle (Δ*Ct*) values normalized to hypoxanthine phosphoribosyltransferase 1 (*Hprt1*) or β2-microglobulin (*B2m*). Primers for *Il6ra* were designed using Primer Blast (http://www.ncbi.nlm.nih.gov/tools/primer-blast) as follows: *Il6ra* forward, 5′-TGCAACGCCATCTGTGAGT-3′; reverse, 5′-CTGGACTTGCTTCCCACACT-3′. Primers for *Sost*, *Hprt1*, and *B2m* have been described previously (27, 48, 58). sIL-6R protein levels were measured in conditioned medium using a sIL-6R ELISA (DuoSet IL-6R-α ELISA kit, R&D Systems (Minneapolis, MN), DY1830) according to the manufacturer's instructions.

Western blotting

Western blotting for phospho-STAT3 was carried out as described previously (27). Whole-cell lysates were prepared from primary calvarial osteoblasts, differentiated for 21 days, or Ocy454 cells differentiated for 14 days in 10-cm^2 dishes. Cultures were serum-starved in 2% fetal bovine serum overnight prior to cytokine treatment. Cells were treated with human IL (hIL)-6 (R&D Systems), human soluble IL (sIL)-6R (R&D Systems), or hyper-IL-6, an IL-6/sIL-6R fusion protein (59), kindly provided by Stefan Rose-John (University of Kiel). Cytokines were provided at the doses indicated in the figure legends for 30 min. Cells were then washed twice with ice-cold PBS before cell lysates were prepared by shaking at 4 °C with modified radioimmune precipitation buffer, proteinase inhibitor (Sigma), and phosphatase inhibitor (Dako, Jena, Denmark), before lysates were centrifuged. Protein concentration was determined as per the manufacturer's protocol (Pierce). 20–50 μg of protein were loaded onto 4–12% gradient gels (Invitrogen) under reducing conditions for electrophoresis before being transferred to nitrocellulose membranes (iBlot, Invitrogen) and probed with antibodies for pSTAT3(Y705) (Cell Signaling Technologies (Danvers, MA), catalog no. 9131, lot 30), STAT3 (Cell Signaling Technologies, catalog no. 9139, lot 8), or panActin Ab-5 (Neomarkers (Portsmouth, NH), catalog no. 1295-P0, lot 1295P1501N). Protein bands were detected with ECL chemiluminescence (GE Healthcare, catalog no. RPN2209) and film (Fujifilm, catalog no. 4741019289) as per the manufacturer's instructions.

Immunohistochemistry

ADAM17 immunostaining was carried out on paraffin-embedded undecalcified tibiae from 16-week-old female C57BL/6 mice by the following method. 5-μm sections were dewaxed in Histoclear, rehydrated through graded ethanols, and endogenous peroxidase–blocked for 30 min in 2% H_2O_2 in TBS. Antigen retrieval was performed by heating samples in 10 mM sodium citrate buffer, pH 6.0, in a Dako cytomation Pascal pressure cooker at 95 °C for 5 min at 2 p.s.i. and then at 90 °C for 2 min before pressure release. Before primary antibody was applied, samples were blocked with 10% swine serum and 10% fetal bovine serum in PBS for 60 min. ADAM17 antibody (Santa Cruz Biotechnology, Inc. (Dallas, TX), SC-13973, 1:50) or IgG control (rabbit IgG, Dako) was applied at 4 °C overnight. After rinsing, a secondary antibody (swine anti-rabbit, Dako) was applied for 30 min at 1:300, followed by streptavidin horseradish peroxidase (Dako) 1:300 in TBS for 30 min and then biotin tyramine at 1:50 in amplification diluent for 10 min (TSA Biotin system kit, PerkinElmer Life Sciences). Samples were rinsed in TBS containing Triton 1000 between each step. Detection was achieved using a diaminobenzidine colorimetric kit (Dako) and counterstained with Mayer's hematoxylin.

In vivo assessment of IL-6 effects on bone formation

To determine whether IL-6 *cis*- or *trans*-signaling can stimulate bone formation *in vivo*, 6-week-old male C57/BL6 mice were subjected to subcutaneous calvarial injections for five consecutive days as described previously (29, 30) with vehicle (saline), hIL-6 alone (0.2 μg/day, hIL-6, R&D Systems), hIL-6 (0.2 μg/day) with sIL-6rα (0.1 μg/day, R&D Systems), hyper-IL-6 (0.2 μg/day, kindly provided by Dr. Rose-John (59), or murine OSM as a positive control (0.2 μg/day) (25). All animal procedures were conducted with approval from the St. Vincent's Health Melbourne Animal Ethics Committee. Ten days after the final injection, calvariae were embedded in methylmethacrylate resin, and sections were cut through the coronal plane for calvarial thickness measurement by histomorphometry, as described previously (30). Measurements were made over 1.48 mm commencing 370 μm on either side of the sagittal suture, at the midpoint between the lambdoid and parietal sutures.

PEPCK-gp130Fc mice

Transgenic mice expressing soluble gp130-Fc under the liver-specific phosphoenolpyruvate carboxykinase promoter (PEPCK-gp130Fc mice) have been described previously by Dr. Rose-John (32). Breeders were kindly provided by Dr. Brendan Jenkins (Hudson Institute, Melbourne, Australia) with the permission of Dr. Rose-John. We carried out two separate studies, as follows. All animal procedures were conducted with approval from the St. Vincent's Health Melbourne Animal Ethics Committee.

We initially bred male and female mice from breeding pairs that were both PEPCK-gp130Fc–transgenic. Serum and femora were collected at 12 weeks of age, as above, and analyzed by micro-CT. Bones from male mice were also tested by three-point bending tests. Because our initial analysis showed reduced body weight and low bone mass in some mice, we measured circulating human sgp130 levels using an ELISA (DuoSet® ELISA, R&D Systems, catalog no. DY228) and stratified the mice into two groups: sgp130Fc^{high} (>10 μg/ml) and

sgp130Fc^{low} (<10 μg/ml) according to Rabe *et al.* (32), where hemizygous transgenic PEPCK-gp130Fc mice had circulating sgp130-Fc levels <10 μg/ml, before further analysis.

Second, to confirm whether hemizygous mice with low circulating sgp130-Fc levels exhibit a bone phenotype, male and female mice were bred from PEPCK-gp130Fc females bred with male C57BL/6 mice to generate only hemizygous or nontransgenic offspring. Serum and femora were collected at 12 weeks of age, and femora were fixed overnight in 4% paraformaldehyde/PBS and stored at room temperature in 70% ethanol until analysis by micro-CT.

Micro-computed tomography and three-point bending tests

Femoral anteroposterior and mediolateral widths were measured at the midpoint, using digital calipers, as described previously. Micro-CT was carried out on femoral samples as described previously (61) using a Skyscan 1076 micro-CT system. Femora were enclosed in plastic tubes and kept moist in gauze swabs soaked in 70% ethanol and scanned at an X-ray potential of 45 kV and a current of 220 μA. Projections were acquired over a rotation step of 0.5 and pixel size of 9 μm. NRecon (version 1.7.4.0, SkyScan) software was used to reconstruct scanned images, with the following parameters: smoothing of 1, a ring artifact reduction of 6, a beam-hardening correction of 35%, and a defect pixel masking of 50%. The samples were then reorientated to measure the same region for each sample using Data Viewer (version 1.4.4). Regions of interest were defined for trabecular and cortical bone using CTAn Analyzer (version 1.15.4.0, SkyScan), as follows. Trabecular bone structure was measured in a region with length 15% of total femoral length, starting 10% proximal to the growth plate (distal metaphysis), and for cortical bone, a 15% long region was measured at a distance 30% proximal to the growth plate. The minimum threshold for trabecular bone was 0.219 mg/cm^3 calcium hydroxyapatite, and for cortical bone, it was 0.632 mg/cm^3 calcium hydroxyapatite. Paraview (version 3.14.1) was used to construct three-dimensional models of trabecular bone structures.

Three-point bending tests were conducted as described previously (61) with a Biodynamic 5500 test instrument (TA Instruments, New Castle, DE). Male bones were tested with a constant span of 10 cm, and the smaller female bones were tested with a span of 9 cm. Before testing, tibiae were kept moist in gauze swabs soaked in PBS. The bone was positioned horizontally with the anterior surface upward, centered on the supports, and the pressing force was directed vertically to the midshaft of the bone. Each bone was compressed at a constant 0.5 mm/s until failure. WinTest software was used to collect the load-displacement data at 250 data points per second for a total of 10 s. Structural properties, including ultimate force, yield force, stiffness, and energy to failure endured by the tibiae, were calculated from load/displacement data (62). The yield point was determined from the load deformation curve at the point at which the curve deviated from linear. Widths of the cortical mid-shaft in the mediolateral and anteroposterior directions, moment of inertia, and average cortical thickness determined by micro-CT were combined with three-point bending data to calculate material-specific properties (63).

Author contributions—N. E. M., M. M., J. E., I. J. P., E. C. W., B. C.-I., and N. A. S. data curation; N. E. M., M. M., J. E., E. C. W., B. C.-I., P. W. M. H., and N. A. S. formal analysis; N. E. M., M. M., J. E., I. J. P., E. C. W., B. C.-I., P. W. M. H., J. H. G., and N. A. S. investigation; N. E. M., M. M., J. E., I. J. P., E. C. W., B. C.-I., P. W. M. H., J. H. G., and N. A. S. methodology; N. E. M., M. M., J. E., I. J. P., E. C. W., B. C.-I., P. W. M. H., J. H. G., T. J. M., and N. A. S. writing-review and editing; J. E., E. C. W., and B. C.-I. visualization; T. J. M. and N. A. S. conceptualization; T. J. M. and N. A. S. supervision; T. J. M. and N. A. S. funding acquisition; N. A. S. writing-original draft; N. A. S. project administration.

Acknowledgments—We thank the staff of the BioResources Centre, St. Vincent's Hospital, Melbourne, for excellent animal care, Brett Tonkin for technical assistance, and Mark Febbraio, Brendan Jenkins, and Stefan Rose-John for their very helpful advice during the planning stages of the study, and for the generous supply of reagents.

References

1. Tamura, T., Udagawa, N., Takahashi, N., Miyaura, C., Tanaka, S., Yamada, Y., Koishihara, Y., Ohsugi, Y., Kumaki, K., and Taga, T. (1993) Soluble interleukin-6 receptor triggers osteoclast formation by interleukin 6. *Proc. Natl. Acad. Sci. U.S.A.* **90,** 11924–11928 CrossRef Medline
2. Roodman, G. D., Kurihara, N., Ohsaki, Y., Kukita, A., Hosking, D., Demulder, A., Smith, J. F., and Singer, F. R. (1992) Interleukin 6: a potential autocrine/paracrine factor in Paget's disease of bone. *J. Clin. Invest.* **89,** 46–52 CrossRef Medline
3. Poli, V., Balena, R., Fattori, E., Markatos, A., Yamamoto, M., Tanaka, H., Ciliberto, G., Rodan, G. A., and Costantini, F. (1994) Interleukin-6 deficient mice are protected from bone loss caused by estrogen depletion. *EMBO J.* **13,** 1189–1196 CrossRef Medline
4. Jilka, R. L., Hangoc, G., Girasole, G., Passeri, G., Williams, D. C., Abrams, J. S., Boyce, B., Broxmeyer, H., and Manolagas, S. C. (1992) Increased osteoclast development after estrogen loss: mediation by interleukin-6. *Science* **257,** 88–91 CrossRef Medline
5. Mitsuyama, K., Toyonaga, A., Sasaki, E., Ishida, O., Ikeda, H., Tsuruta, O., Harada, K., Tateishi, H., Nishiyama, T., and Tanikawa, K. (1995) Soluble interleukin-6 receptors in inflammatory bowel disease: relation to circulating interleukin-6. *Gut* **36,** 45–49 CrossRef Medline
6. Kotake, S., Sato, K., Kim, K. J., Takahashi, N., Udagawa, N., Nakamura, I., Yamaguchi, A., Kishimoto, T., Suda, T., and Kashiwazaki, S. (1996) Interleukin-6 and soluble interleukin-6 receptors in the synovial fluids from rheumatoid arthritis patients are responsible for osteoclast-like cell formation. *J. Bone Miner. Res.* **11,** 88–95 CrossRef Medline
7. Wong, P. K., Quinn, J. M., Sims, N. A., van Nieuwenhuijze, A., Campbell, I. K., and Wicks, I. P. (2006) Interleukin-6 modulates production of T lymphocyte-derived cytokines in antigen-induced arthritis and drives inflammation-induced osteoclastogenesis. *Arthritis Rheum.* **54,** 158–168 CrossRef Medline
8. Kyrtsonis, M. C., Dedoussis, G., Zervas, C., Perifanis, V., Baxevanis, C., Stamatelou, M., and Maniatis, A. (1996) Soluble interleukin-6 receptor (sIL-6R), a new prognostic factor in multiple myeloma. *Br. J. Haematol.* **93,** 398–400 CrossRef Medline
9. Scheller, J., Garbers, C., and Rose-John, S. (2014) Interleukin-6: from basic biology to selective blockade of pro-inflammatory activities. *Semin. Immunol.* **26,** 2–12 Medline
10. Gao, Y., Morita, I., Maruo, N., Kubota, T., Murota, S., and Aso, T. (1998) Expression of IL-6 receptor and GP130 in mouse bone marrow cells during osteoclast differentiation. *Bone* **22,** 487–493 CrossRef Medline
11. Suda, T., Udagawa, N., Nakamura, I., Miyaura, C., and Takahashi, N. (1995) Modulation of osteoclast differentiation by local factors. *Bone* **17,** 87S–91S CrossRef Medline
12. Richards, C. D., Langdon, C., Deschamps, P., Pennica, D., and Shaughnessy, S. G. (2000) Stimulation of osteoclast differentiation *in vitro* by mouse oncostatin M, leukaemia inhibitory factor, cardiotrophin-1 and

interleukin 6: synergy with dexamethasone. *Cytokine* **12,** 613–621 CrossRef Medline

13. Horwood, N. J., Elliott, J., Martin, T. J., and Gillespie, M. T. (1998) Osteotropic agents regulate the expression of osteoclast differentiation factor and osteoprotegerin in osteoblastic stromal cells. *Endocrinology* **139,** 4743–4746 CrossRef Medline
14. Littlewood, A. J., Russell, J., Harvey, G. R., Hughes, D. E., Russell, R. G., and Gowen, M. (1991) The modulation of the expression of IL-6 and its receptor in human osteoblasts *in vitro*. *Endocrinology* **129,** 1513–1520 CrossRef Medline
15. Bellido, T., Borba, V. Z., Roberson, P., and Manolagas, S. C. (1997) Activation of the Janus kinase/STAT (signal transducer and activator of transcription) signal transduction pathway by interleukin-6-type cytokines promotes osteoblast differentiation. *Endocrinology* **138,** 3666–3676 CrossRef Medline
16. Bellido, T., Stahl, N., Farruggella, T. J., Borba, V., Yancopoulos, G. D., and Manolagas, S. C. (1996) Detection of receptors for interleukin-6, interleukin-11, leukemia inhibitory factor, oncostatin M, and ciliary neurotrophic factor in bone marrow stromal/osteoblastic cells. *J. Clin. Invest.* **97,** 431–437 CrossRef Medline
17. Nishimura, R., Moriyama, K., Yasukawa, K., Mundy, G. R., and Yoneda, T. (1998) Combination of interleukin-6 and soluble interleukin-6 receptors induces differentiation and activation of JAK-STAT and MAP kinase pathways in MG-63 human osteoblastic cells. *J. Bone Miner. Res.* **13,** 777–785 CrossRef Medline
18. Li, Y., Bäckesjö, C. M., Haldosén, L. A., and Lindgren, U. (2008) IL-6 receptor expression and IL-6 effects change during osteoblast differentiation. *Cytokine* **43,** 165–173 CrossRef Medline
19. Dame, J. B., and Juul, S. E. (2000) The distribution of receptors for the pro-inflammatory cytokines interleukin (IL)-6 and IL-8 in the developing human fetus. *Early Hum. Dev.* **58,** 25–39 CrossRef Medline
20. Wu, A. C., Kidd, L. J., Cowling, N. R., Kelly, W. L., and Forwood, M. R. (2014) Osteocyte expression of caspase-3, COX-2, IL-6 and sclerostin are spatially and temporally associated following stress fracture initiation. *BoneKEy Reports* **3,** 571 CrossRef Medline
21. Bakker, A. D., Kulkarni, R. N., Klein-Nulend, J., and Lems, W. F. (2014) IL-6 alters osteocyte signaling toward osteoblasts but not osteoclasts. *J. Dent. Res.* **93,** 394–399 CrossRef Medline
22. Johnson, R. W., Brennan, H. J., Vrahnas, C., Poulton, I. J., McGregor, N. E., Standal, T., Walker, E. C., Koh, T. T., Nguyen, H., Walsh, N. C., Forwood, M. R., Martin, T. J., and Sims, N. A. (2014) The primary function of gp130 signaling in osteoblasts is to maintain bone formation and strength, rather than promote osteoclast formation. *J. Bone Miner. Res.* **29,** 1492–1505 CrossRef Medline
23. Xiong, J., Onal, M., Jilka, R. L., Weinstein, R. S., Manolagas, S. C., and O'Brien, C. A. (2011) Matrix-embedded cells control osteoclast formation. *Nat. Med.* **17,** 1235–1241 CrossRef Medline
24. Nakashima, T., Hayashi, M., Fukunaga, T., Kurata, K., Oh-Hora, M., Feng, J. Q., Bonewald, L. F., Kodama, T., Wutz, A., Wagner, E. F., Penninger, J. M., and Takayanagi, H. (2011) Evidence for osteocyte regulation of bone homeostasis through RANKL expression. *Nat. Med.* **17,** 1231–1234 CrossRef Medline
25. Walker, E. C., McGregor, N. E., Poulton, I. J., Solano, M., Pompolo, S., Fernandes, T. J., Constable, M. J., Nicholson, G. C., Zhang, J. G., Nicola, N. A., Gillespie, M. T., Martin, T. J., and Sims, N. A. (2010) Oncostatin M promotes bone formation independently of resorption when signaling through leukemia inhibitory factor receptor in mice. *J. Clin. Invest.* **120,** 582–592 CrossRef Medline
26. Dallas, D. J., Genever, P. G., Patton, A. J., Millichip, M. I., McKie, N., and Skerry, T. M. (1999) Localization of ADAM10 and notch receptors in bone. *Bone* **25,** 9–15 CrossRef Medline
27. Walker, E. C., Johnson, R. W., Hu, Y., Brennan, H. J., Poulton, I. J., Zhang, J. G., Jenkins, B. J., Smyth, G. K., Nicola, N. A., and Sims, N. A. (2016) Murine oncostatin M acts via leukemia inhibitory factor receptor to phosphorylate signal transducer and activator of transcription 3 (STAT3) but not STAT1, an effect that protects bone mass. *J. Biol. Chem.* **291,** 21703–21716 CrossRef Medline
28. Spatz, J. M., Wein, M. N., Gooi, J. H., Qu, Y., Garr, J. L., Liu, S., Barry, K. J., Uda, Y., Lai, F., Dedic, C., Balcells-Camps, M., Kronenberg, H. M., Babij, P., and Pajevic, P. D. (2015) The Wnt inhibitor sclerostin is up-regulated by mechanical unloading in osteocytes *in vitro*. *J. Biol. Chem.* **290,** 16744–16758 CrossRef Medline
29. Cornish, J., Callon, K., King, A., Edgar, S., and Reid, I. R. (1993) The effect of leukemia inhibitory factor on bone *in vivo*. *Endocrinology* **132,** 1359–1366 CrossRef Medline
30. Walker, E. C., McGregor, N. E., Poulton, I. J., Pompolo, S., Allan, E. H., Quinn, J. M., Gillespie, M. T., Martin, T. J., and Sims, N. A. (2008) Cardiotrophin-1 is an osteoclast-derived stimulus of bone formation required for normal bone remodeling. *J. Bone Miner. Res.* **23,** 2025–2032 CrossRef Medline
31. Rakemann, T., Niehof, M., Kubicka, S., Fischer, M., Manns, M. P., Rose-John, S., and Trautwein, C. (1999) The designer cytokine hyper-interleukin-6 is a potent activator of STAT3-dependent gene transcription *in vivo* and *in vitro*. *J. Biol. Chem.* **274,** 1257–1266 CrossRef Medline
32. Rabe, B., Chalaris, A., May, U., Waetzig, G. H., Seegert, D., Williams, A. S., Jones, S. A., Rose-John, S., and Scheller, J. (2008) Transgenic blockade of interleukin 6 transsignaling abrogates inflammation. *Blood* **111,** 1021–1028 CrossRef Medline
33. Müllberg, J., Schooltink, H., Stoyan, T., Günther, M., Graeve, L., Buse, G., Mackiewicz, A., Heinrich, P. C., and Rose-John, S. (1993) The soluble interleukin-6 receptor is generated by shedding. *Eur. J. Immunol.* **23,** 473–480 CrossRef Medline
34. Matthews, V., Schuster, B., Schütze, S., Bussmeyer, I., Ludwig, A., Hundhausen, C., Sadowski, T., Saftig, P., Hartmann, D., Kallen, K. J., and Rose-John, S. (2003) Cellular cholesterol depletion triggers shedding of the human interleukin-6 receptor by ADAM10 and ADAM17 (TACE). *J. Biol. Chem.* **278,** 38829–38839 CrossRef Medline
35. Garbers, C., Jänner, N., Chalaris, A., Moss, M. L., Floss, D. M., Meyer, D., Koch-Nolte, F., Rose-John, S., and Scheller, J. (2011) Species specificity of ADAM10 and ADAM17 proteins in interleukin-6 (IL-6) trans-signaling and novel role of ADAM10 in inducible IL-6 receptor shedding. *J. Biol. Chem.* **286,** 14804–14811 CrossRef Medline
36. Hall, K. C., Hill, D., Otero, M., Plumb, D. A., Froemel, D., Dragomir, C. L., Maretzky, T., Boskey, A., Crawford, H. C., Selleri, L., Goldring, M. B., and Blobel, C. P. (2013) ADAM17 controls endochondral ossification by regulating terminal differentiation of chondrocytes. *Mol. Cell. Biol.* **33,** 3077–3090 CrossRef Medline
37. Dreymueller, D., Theodorou, K., Donners, M., and Ludwig, A. (2017) Fine tuning cell migration by a disintegrin and metalloproteinases. *Mediators Inflamm.* **2017,** 9621724–9621724 CrossRef Medline
38. Honda, M., Yamamoto, S., Cheng, M., Yasukawa, K., Suzuki, H., Saito, T., Osugi, Y., Tokunaga, T., and Kishimoto, T. (1992) Human soluble IL-6 receptor: its detection and enhanced release by HIV infection. *J. Immunol.* **148,** 2175–2180 Medline
39. Schaffler, M. B., Cheung, W. Y., Majeska, R., and Kennedy, O. (2014) Osteocytes: master orchestrators of bone. *Calcif. Tissue Int.* **94,** 5–24 CrossRef Medline
40. Girasole, G., Giuliani, N., Modena, A. B., Passeri, G., and Pedrazzoni, M. (1999) Oestrogens prevent the increase of human serum soluble interleukin-6 receptor induced by ovariectomy *in vivo* and decrease its release in human osteoblastic cells *in vitro*. *Clin. Endocrinol.* **51,** 801–807 CrossRef Medline
41. Lazzaro, L., Tonkin, B. A., Poulton, I. J., McGregor, N. E., Ferlin, W., and Sims, N. A. (2018) IL-6 trans-signalling mediates trabecular, but not cortical, bone loss after ovariectomy. *Bone* **112,** 120–127 CrossRef Medline
42. Sims, N. A., Jenkins, B. J., Nakamura, A., Quinn, J. M., Li, R., Gillespie, M. T., Ernst, M., Robb, L., and Martin, T. J. (2005) Interleukin-11 receptor signaling is required for normal bone remodeling. *J. Bone Miner. Res.* **20,** 1093–1102 CrossRef Medline
43. Johnson, R. W., McGregor, N. E., Brennan, H. J., Crimeen-Irwin, B., Poulton, I. J., Martin, T. J., and Sims, N. A. (2015) Glycoprotein130 (Gp130)/interleukin-6 (IL-6) signalling in osteoclasts promotes bone formation in periosteal and trabecular bone. *Bone* **81,** 343–351 CrossRef Medline
44. Kartsogiannis, V., Zhou, H., Horwood, N. J., Thomas, R. J., Hards, D. K., Quinn, J. M., Niforas, P., Ng, K. W., Martin, T. J., and Gillespie, M. T.

(1999) Localization of RANKL (receptor activator of NFκB ligand) mRNA and protein in skeletal and extraskeletal tissues. *Bone* **25,** 525–534 CrossRef Medline

45. Udagawa, N., Takahashi, N., Katagiri, T., Tamura, T., Wada, S., Findlay, D. M., Martin, T. J., Hirota, H., Taga, T., Kishimoto, T., and Suda, T. (1995) Interleukin (IL)-6 induction of osteoclast differentiation depends on IL-6 receptors expressed on osteoblastic cells but not on osteoclast progenitors. *J. Exp. Med.* **182,** 1461–1468 CrossRef Medline
46. Schlöndorff, J., Lum, L., and Blobel, C. P. (2001) Biochemical and pharmacological criteria define two shedding activities for TRANCE/OPGL that are distinct from the tumor necrosis factor α convertase. *J. Biol. Chem.* **276,** 14665–14674 CrossRef Medline
47. Hikita, A., Yana, I., Wakeyama, H., Nakamura, M., Kadono, Y., Oshima, Y., Nakamura, K., Seiki, M., and Tanaka, S. (2006) Negative regulation of osteoclastogenesis by ectodomain shedding of receptor activator of NF-κB ligand. *J. Biol. Chem.* **281,** 36846–36855 CrossRef Medline
48. Chia, L. Y., Walsh, N. C., Martin, T. J., and Sims, N. A. (2015) Isolation and gene expression of haematopoietic-cell-free preparations of highly purified murine osteocytes. *Bone* **72,** 34–42 CrossRef Medline
49. Jostock, T., Müllberg, J., Ozbek, S., Atreya, R., Blinn, G., Voltz, N., Fischer, M., Neurath, M. F., and Rose-John, S. (2001) Soluble gp130 is the natural inhibitor of soluble interleukin-6 receptor transsignaling responses. *Eur. J. Biochem.* **268,** 160–167 CrossRef Medline
50. Garbers, C., Thaiss, W., Jones, G. W., Waetzig, G. H., Lorenzen, I., Guilhot, F., Lissilaa, R., Ferlin, W. G., Grötzinger, J., Jones, S. A., Rose-John, S., and Scheller, J. (2011) Inhibition of classic signaling is a novel function of soluble glycoprotein 130 (sgp130), which is controlled by the ratio of interleukin 6 and soluble interleukin 6 receptor. *J. Biol. Chem.* **286,** 42959–42970 CrossRef Medline
51. Atreya, R., Mudter, J., Finotto, S., Müllberg, J., Jostock, T., Wirtz, S., Schutz, M., Bartsch, B., Holtmann, M., Becker, C., Strand, D., Czaja, J., Schlaak, J. F., Lehr, H. A., Autschbach, F., *et al.* (2000) Blockade of interleukin 6 trans signaling suppresses T-cell resistance against apoptosis in chronic intestinal inflammation: evidence in Crohn disease and experimental colitis *in vivo*. *Nat. Med.* **6,** 583–588 CrossRef Medline
52. Rose-John, S. (2017) The soluble interleukin 6 receptor: advanced therapeutic options in inflammation. *Clin. Pharmacol. Ther.* **102,** 591–598 CrossRef Medline
53. Poulton, I. J., McGregor, N. E., Pompolo, S., Walker, E. C., and Sims, N. A. (2012) Contrasting roles of leukemia inhibitory factor in murine bone development and remodeling involve region-specific changes in vascularization. *J. Bone Miner. Res.* **27,** 586–595 CrossRef Medline
54. Martin, T. J., Ng, K. W., Partridge, N. C., and Livesey, S. A. (1987) Hormonal influences on bone cells. *Methods Enzymol.* **145,** 324–336 CrossRef Medline
55. Deleted in proof
56. Allan, E. H., Ho, P. W., Umezawa, A., Hata, J., Makishima, F., Gillespie, M. T., and Martin, T. J. (2003) Differentiation potential of a mouse bone marrow stromal cell line. *J. Cell. Biochem.* **90,** 158–169 CrossRef Medline
57. Quinn, J. M., Sims, N. A., Saleh, H., Mirosa, D., Thompson, K., Bouralexis, S., Walker, E. C., Martin, T. J., and Gillespie, M. T. (2008) IL-23 inhibits osteoclastogenesis indirectly through lymphocytes and is required for the maintenance of bone mass in mice. *J. Immunol.* **181,** 5720–5729 CrossRef Medline
58. Kartsogiannis, V., Sims, N. A., Quinn, J. M., Ly, C., Cipetic, M., Poulton, I. J., Walker, E. C., Saleh, H., McGregor, N. E., Wallace, M. E., Smyth, M. J., Martin, T. J., Zhou, H., Ng, K. W., and Gillespie, M. T. (2008) Osteoclast inhibitory lectin, an immune cell product that is required for normal bone physiology *in vivo*. *J. Biol. Chem.* **283,** 30850–30860 CrossRef Medline
59. Fischer, M., Goldschmitt, J., Peschel, C., Brakenhoff, J. P., Kallen, K. J., Wollmer, A., Grötzinger, J., and Rose-John, S. (1997) I. A bioactive designer cytokine for human hematopoietic progenitor cell expansion. *Nat. Biotechnol.* **15,** 142–145 CrossRef Medline
60. Deleted in proof
61. Cho, D. C., Brennan, H. J., Johnson, R. W., Poulton, I. J., Gooi, J. H., Tonkin, B. A., McGregor, N. E., Walker, E. C., Handelsman, D. J., Martin, T. J., and Sims, N. A. (2017) Bone corticalization requires local SOCS3 activity and is promoted by androgen action via interleukin-6. *Nat. Commun.* **8,** 806 CrossRef Medline
62. Jepsen, K. J., Silva, M. J., Vashishth, D., Guo, X. E., and van der Meulen, M. C. (2015) Establishing biomechanical mechanisms in mouse models: practical guidelines for systematically evaluating phenotypic changes in the diaphyses of long bones. *J. Bone Miner. Res.* **30,** 951–966 CrossRef Medline
63. Turner, C. H., and Burr, D. B. (1993) Basic biomechanical measurements of bone: a tutorial. *Bone* **14,** 595–608 CrossRef Medline